1639

Analysis of the Joint Structure of the Vehicle Body by Condensed Joint Matrix Method

Myung-Won Suh, Won-Ho Yang
Professor, School of Mechanical Engineering, Sungkyunkwan University,
300 Chunchun-dong, Jangan-ku, Suwon, Kyoungki-do 440-746, Korea
Jonghwan Suhr*
Researcher, Safety and Structural Integrity Research Center, Sungkyunkwan University,
300 Chunchun-dong, Jangan-ku, Suwon, Kyoungki-do 440-746, Korea

It is often necessary that the joint characteristics should be determined in the early stage of the vehicle body design. The researches on identification of joints in a vehicle body have been performed until the recent year. In this study, the joint characteristics of vehicle structure were expressed as the condensed matrix forms from the full joint stiffness matrix. The condensed joint stiffness matrix was applied to typical T-type and Edge-type joints, and the usefulness was confirmed. In addition, it was applied to the real center pillar model and the full vehicle body in order to validate the practical application.

Key Words : Joint Characteristics, Joint Stiffness Matrix, Condensed Joint Matrix

1. Introduction

A vehicle body structure has the various joints that are complicatedly connected. The pillar, the roof rail and the rocker are the typical joints in vehicle body structure. These joints consist of the inner panels, the outer panels and the reinforcements, which are connected by spot welding. It is well known that the joint characteristics can impact on the static and the dynamic behavior of the vehicle structure.

In order to identify and express these joint characteristics, Chang (1974) studied to represent the flexibility of body connections, or joints, using torsional spring element. It is a conventional analysis technique that is based on the rigid connections only, neglecting its flexibility. It was

* Corresponding Author,
  E-mail : suhr@dreamwiz.com
  TEL : +82-31-290-7502; **FAX :** +82-31-290-5276
  Researcher, Safety and Structural Integrity Research Center, Sungkyunkwan University, 300 Chunchun -dong, Jangan-ku, Suwon, Kyoungki-do 440-746, Korea. (Manuscript **Received** March 20, 2001; **Revised** October 5, 2001)

found that it could result in almost 50% error when the stiffness of the whole vehicle body structure is calculated. Moon et al. (1995) studied on the calculation technique of the torsional spring constants through a static test, in order to consider the flexibility of the joint. They discussed that the torsional spring constants, which were calculated from the experiment, could be improved, in turn, by a sensitivity analysis. Although this approach has been commonly adopted until now, the significant error could be involved. I think the reasons are as follows. Like above approach, if the joint characteristics are represented with scalar springs only, the only diagonal terms would be considered in the stiffness matrix, while the coupled terms would be ignored.

Moreover, not only it isn't easy to determine the spring constants from the displacements corresponding to the pre-assigned loads in the static test, but also those displacements mostly involve the effect of the desired load as well as other loads, which are not desired.

Some research efforts were diverted from representing the joint characteristics into the scalar

springs. Kim, et al. (1995) studied how to derive the joint stiffness matrix considering the flexibility of the T-type joint, which has a box cross-section. This idea was fundamentally based on the strain energy concept. They defined the joint compliance matrix from the relationship between a moment and its rotational degree of freedom. The joint compliance matrix was calculated by differentiating the strain energy of the joint part with respect to the external moments. The joint stiffness matrix can be obtained from the inverse of this joint compliance matrix. However, the application of the method is limited to the joint structure that has a simple cross-section such as a box shape. The joint structures in vehicle, which have very complicated cross-section make a practical application more difficult and cumbersome. Katakami, et al. (1990) derived the joint stiffness matrix for much more general joint structure. Two different finite element models were built for a joint structure in order to obtain the joint stiffness matrix. One was a detailed joint model using shell element, the other was a simplified joint model using beam element with rigid joint. It is natural that there should be differences of stiffness between these two models. In order to derive stiffness matrices of the two models, FE analyses were necessary. The displacements, especially the rotational ones, corresponding to assigned load were calculated.

The above two methods are based on the relationship between the various load sets and these displacements. A number of calculations and FE analyses are required. It seems that these are too intricate to apply to the practical problems.

Although the various studies have been performed until recent years, the difficulty and the complexity of the procedures have hindered the practical application to the vehicle body structure. In this study, a practical method for identifying and expressing the joint characteristics in complete matrix form is presented. The calculations of displacements corresponding to pre-assigned loads are not necessary. The joint characteristics of the vehicle body structure can be very easily expressed in the condensed matrix form. A joint stiffness matrix is derived. The

usefulness of this approach is confirmed by the various example problems including the body structure of the passenger vehicle.

2. Condensation

Very often some of DOFs are of only secondary importance. The analysis may, therefore, be carried out more efficiently if unwanted DOFs can be eliminated by some procedure while maintaining the acceptable accuracy. Condensation is the process of reducing the number of DOFs. It involves a reformulation of the stiffness and the mass matrices based on partitions of a stiffness matrix. Guyan(1965) expanded "static condensation" into dynamic problem fields.

Consider the equation of free vibration

$$[M]\{\ddot{u}\}+[K]\{u\}=\{0\} \qquad (1)$$

Total degree of freedom $\{u\}$ are partitioned into a set $\{u_a\}$ termed master degree of freedom, which are to be retained for the analysis, and a set $\{u_o\}$ termed slave degree of freedom, which are to be eliminated.

Partitioning $[M]$ and $[K]$ in a compatible manner, Eq. (1) becomes

$$\begin{bmatrix}[M_{aa}] & [M_{ao}] \\ [M_{oa}] & [M_{oo}]\end{bmatrix}\begin{Bmatrix}\ddot{u}_a \\ \ddot{u}_o\end{Bmatrix}+\begin{bmatrix}[K_{aa}] & [K_{ao}] \\ [K_{oa}] & [K_{oo}]\end{bmatrix}\begin{Bmatrix}u_a \\ u_o\end{Bmatrix}=\{0\} \qquad (2)$$

From the second of the two matrix Eq. in (2), the assumption is made that the relationship between $\{u_o\}$ and $\{u_a\}$ is not affected by the inertia terms. In other words, slave DOFs are assumed to move quasi-statically in response to the motion of master DOFs. Thus, Equation now reduces to

$$\lfloor K_{oa}\rfloor \{u_a\}\lfloor K_{oo}\rfloor \{u_o\}=\{0\} \qquad (3)$$

Solving for $\{u_o\}$ gives

$$\{u_o\}=-[K_{oo}]^{-1}[K_{oa}]\{u_a\} \qquad (4)$$

Therefore

$$\{u\}=\begin{Bmatrix}u_a \\ u_o\end{Bmatrix}=\begin{bmatrix}I \\ -[K_{oo}]^{-1}[K_{oa}]\end{bmatrix}\{u_a\}=[R]\{u_a\} \qquad (5)$$

The kinetic and strain energy of the system are

$$T=\frac{1}{2}\{\dot{u}_a\}^T[M]^R\{\dot{u}_a\} \qquad (6)$$

$$U = \frac{1}{2}\{ u_a \}^T [K]^R \{ u_a \} \qquad (7)$$

where

$$[M]^R = [R]^T [M][R], \ [K]^R = [R]^T [K][R] \quad (8)$$

Substituting $[R]$ of (5) into (8) gives

$$[K]^R = [K_{aa}] - [K_{ao}] - [K_{oo}]^{-1}[K_{oa}] \qquad (9)$$

$$[M]^R = [M_{aa}] - [M_{ao}][K_{oo}]^{-1}[K_{oa}] - [K_{ao}]$$
$$[K_{oo}]^{-1}[M_{oa}] + [K_{ao}][K_{oo}]^{-1}[M_{oo}][K_{oo}]^{-1}[K_{oa}] \quad (10)$$

Substituting (6), (7) into Lagrange's equation gives

$$[M]^R \{ \ddot{u}_a \} + [K]^R \{ u_a \} = \{ 0 \} \qquad (11)$$

as the equation of motion.

$[K]^R$, $[M]^R$ is symmetric matrix. Though $[K]$ is a banded matrix and $[M]$ is a diagonal matrix, $[K]^R$ and $[M]^R$ are the full matrices. With respect to the selection of the master DOFs, G. C. Wright and G. A. Miles(1971) suggested that the slave DOFs should be chosen in the region of large stiffness and the master DOFs should be selected in regions of large flexibility to have more accurate solution.

3. CJM (Condensed Joint Matrix) Method

In this section, the method for calculating the joint characteristic matrix from the full joint matrix using condensation is explained. Firstly, the joint with three branch members is considered. The joint is modeled by shell elements as shown in Fig. 1. All the nodes at the end of branch i are subjected to one imaginary point, Pi, such as Fig. 1. It is assumed that each imaginary point, Pi has only three rotational DOFs (θ_x, θ_y,
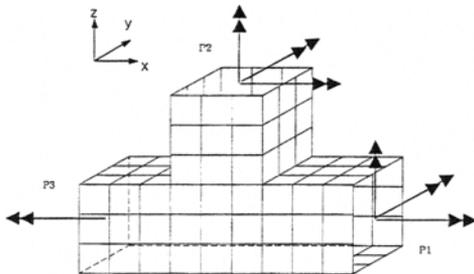
Fig. 1   The joint with shell elements

θ_z)

In order to apply the condensation to the joint model, the total DOFs have to be partitioned into master DOFs and slave DOFs. Many research papers[1], [2], [3], [4], [6] have shown that the rotational stiffness in joint part has a dominant effect on the behavior of a joint structure. Thus, all the rotational DOFs, which are activated on the imaginary point, Pi are selected as master DOFs for each branch member. The other DOFs on the joint structure modeled with shell elements are selected as slave DOFs. The number of master DOFs would be 9 in this case of Fig. 1, such as Eq. (12).

$$\{ \theta \}_{master} = [\theta^{(1)}_x, \ \theta^{(1)}_y, \ \theta^{(1)}_z, \ \theta^{(2)}_x, \ \theta^{(2)}_y, \ \theta^{(2)}_z,$$
$$\theta^{(3)}_x, \ \theta^{(3)}_y, \ \theta^{(3)}_z]^T \qquad (12)$$

where superscript (1), (2), (3) indicate the branch number and x, y, z are the coordinate axes.

From Eq. (1) to (9), 9 x 9 condensed joint stiffness matrix can be expressed from the full joint stiffness matrix, as follows.

$$[K]_J = \begin{pmatrix} [K_{11}] & [K_{12}] & [K_{13}] \\ [K_{21}] & [K_{22}] & [K_{23}] \\ [K_{31}] & [K_{32}] & [K_{33}] \end{pmatrix} \qquad (13)$$

where $[K_{11}]$, $[K_{12}]$, $\cdots$ $[K_{33}]$ are 3 x 3 matrix and the subscript 1, 2 3, denote the branch number.

Similarly, 9 x 9 condensed joint mass matrix can be expressed from the full joint mass matrix from Eq. (10).

$$[M]_J = \begin{pmatrix} [M_{11}] & [M_{12}] & [M_{13}] \\ [M_{21}] & [M_{22}] & [M_{23}] \\ [M_{31}] & [M_{32}] & [M_{33}] \end{pmatrix} \qquad (14)$$

The joint characteristics are obtained as the condensed form from the full stiffness matrix and mass matrix. In this study, the proposed method is called as CJM (Condensed Joint Matrix) method. In this method, the calculation of the displacements corresponding to the assigned loads is not necessary to formulate the joint matrix. The joint characteristics of a vehicle body structure, which has the complicate shapes, can be very easily expressed in the condensed matrix form. In addition, not only the joint stiffness matrix, but also the joint mass matrix can be obtained.
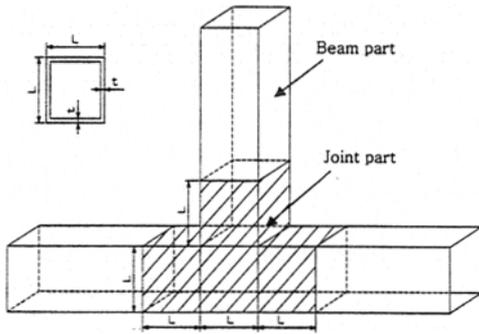
Fig. 2   The T-type joint structure
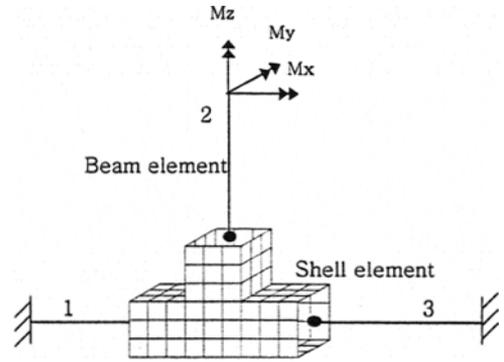
Fig. 3   A detailed joint model with shell elements

4. Application of CJM to T-type Joint Structure

T-type joint structure, which has a box section, is considered as the first application. The joint structure can be divided by two parts as shown in Fig. 2, which is the joint part which don't have to be modeled by straight beam for its flexibility, and the beam part which can be assumed by constant-area-beam for a general membrane. Three different finite element models for T-type joint structure are built to evaluate the static and the dynamic stiffness. One is a detailed joint model. Its joint part is modeled with shell element and its beam part is modeled with beam element. It is called "shell model", as shown in Fig. 3. The second is a simplified joint model using only beam element with rigid joint. It is called "rigid model", and both the joint part and the beam part are modeled with beam element, as shown Fig. 4. The third, called "CJM model", is a proposed joint model using CJM method, as shown Fig. 5. The joint part is modeled with the condensed joint characteristic matrix. This matrix is derived from the joint part modeled with shell element. The beam part is modeled with beam element, in the same way as the above two joint models. NASTRAN Ver. 68 was used and the shell models and the rigid models were modeled respectively by QUAD4 and TRIA3 elements, and BEAM elements.

To analyze the static stiffness, each tip of branch 1 and 3 are fixed, and moments (Mx, My,
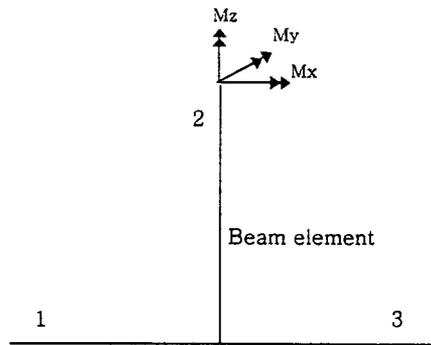
Fig. 4   A simplified joint model with beam elements
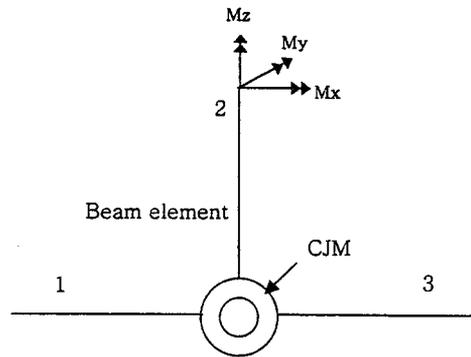
Fig. 5   A proposed joint model with CJM

Mz) are applied to the tip of branch 2, as shown in Fig. 3. The analysis results of the static stiffness are listed in Table 1. The rigid model has max. 9% larger static stiffness than shell model while the CJM model has the trivial errors within 2% in comparison with shell model. To analyze the

Table 1 Normalized displacement of T-type joint structure for static stiffness

	Shell model	Rigid model (error)	CJM model (error)
$\theta_x/\{\theta_x\}_s$	1.0	0.954(4.6%)	1.0(0%)
$\theta_y/\{\theta_y\}_s$	1.0	0.910(9.0%)	1.019(−1.9%)
$\theta_z/\{\theta_z\}_s$	1.0	0.972(2.8%)	1.017(−1.7%)

Table 2 Natural frequency (Hz) of T-type joint structure for dynamic stiffness

Mode	Shell model	Rigid model (error)	CJM model (error)
1st	157.7	179.1(13.6%)	152.3(−3.4%)
2nd	250.4	263.6(5.0%)	251.1(0.3%)
3rd	306.9	298.3(−2.8%)	325.3(6.0%)

Table 3 Normalized displacement of Edge-type joint structure for static stiffness

	Shell model	Rigid model (error)	CJM model (error)
$\theta_x/\{\theta_x\}_s$	1.0	0.889(11.0%)	0.997(0.3%)
$\theta_y/\{\theta_y\}_s$	1.0	0.890(11.0%)	0.892(11.0%)
$\theta_z/\{\theta_z\}_s$	1.0	1.014(1.4%)	0.992(0.8%)

Table 4 Natural frequency (Hz) of Edge-type joint structure for dynamic stiffness

Mode	Shell model	Rigid model (error)	CJM model (error)
1st	141.6	161.2(13.8%)	138.1(−2.5%)
2nd	159.9	181.9(13.8%)	155.1(−3.0%)
3rd	167.8	206.4(23.0%)	166.8(−0.6%)

dynamic stiffness, all the boundary conditions are set to be free. The natural frequencies, which may be considered as the dynamic stiffness, are listed in Table 2. All of the three models have the same mode shape in each natural mode. The rigid model has approximately 14% larger natural frequency than shell model in the 1st natural mode, while the CJM model's natural frequencies have the slight errors within 6% in comparison with shell model. Table 1 and 2 show very good correlation between shell and CJM model in both static and dynamic response.

The general trend, that a simplified joint model using only beam element has a larger static and dynamic stiffness than a detailed joint model using shell elements, is verified.

5. Application of CJM to Edge-type Joint Sturcture

Edge-type joint structure, which has a box section, is considered as the second application. The joint structure can be divided by two parts as in Fig. 6. As for the T-type joint structure, three different finite element models, which are shell model, rigid model and CJM model, are built for Edge-type joint structure to evaluate the static and the dynamic stiffness.

The analysis results of the static and dynamic stiffness are listed in Table 3, and 4. Tables 3 and

Fig. 6 The Corner-type joint structure

4 show the same tendency as Tables 1 and 2, respectively. All of the three models have the same mode shape in each natural mode. The rigid model has approximately 23.0% larger natural frequency than shell model in the 3rd natural mode, while the CJM model's natural frequencies have the negligible errors within −0.6% in comparison with shell model.

6. Application of CJM to Center Pillar of Passenger Car

The actual center pillar of the passenger car is considered as the third application. Three different finite element models are built to evaluate

Table 5 The model features of the center pillar model

	Shell model	Rigid model	CJM model
Total number of DOFs	7393	192	222

Table 6 Normalized displacement of lower center pillar for static stiffness

	Shell model	Rigid model (error)	CJM model (error)
$\theta_x/\{\theta_x\}_s$	1.0	8.862e-05 (—)	1.028 (−2.8%)
$\theta_y/\{\theta_y\}_s$	1.0	0.151 (84.9%)	1.087 (−8.7%)
$\theta_z/\{\theta_z\}_s$	1.0	1.545e-02 (—)	1.067 (−6.7%)

Table 7 Natural frequency (Hz) of lower center pillar for dynamic stiffness

Mode	Shell model	Rigid model (error)	CJM model (error)
1st	1.51	1.98(31.1%)	1.34(−11.3%)
2nd	2.42	—	2.34(−3.3%)
3rd	2.89	3.18(10.0%)	2.82(−2.4%)

Fig. 7 A detailed lower center pillar model of passenger car with shell elements

static and dynamic stiffness, as listed in Table 5. The actual center pillar is divided by the joint part, and the beam part which can be assumed by constant-area-beam as shown in Fig. 7. The joint part of a detailed pillar model is modeled with 2, 422 rectangular and 363 triangular shell elements. The spot-welding part is modeled with rigid elements.

The analysis results of the static stiffness are listed in Table 6. The boundary condition is determined and each moment (Mx, My, Mz) is applied, similarly to Fig. 3 or T-type joint structure application. The CJM model has much fewer DOFs than shell model, which are 222 and 7,393, respectively. The CJM model has the slight errors within 9%, while the rigid model has much larger static stiffness than shell model. The rigid model shows excessively stiff results. The natural frequencies with the free boundary condition are listed in Table 7. The analysis results of the natural frequencies and the mode shapes show

good correlation between shell and CJM model. Even though the CJM model has much fewer DOFs than shell model, the rigid model has approximately 31% larger natural frequency than shell model in the 1st natural mode, while the CJM model has the reasonable errors within 10%.

It is verified that it isn't good for the rigid model to be applied to the practical problem, because of the complex cross sections and the crooked curvatures of a real center pillar model.

7. Application of CJM to Body Vehicle Structure

The vehicle body structure is considered as the final application. There are total 4 center pillars in the vehicle body structure, as shown in Fig. 8. The condensed joint stiffness matrix is derived from each center pillar model by using CJM method. As for the above applications, three different finite element vehicle models are built to solve natural frequencies and mode shape, as listed in Table 8. The bending and twisting mode, which are considered as the decisive behaviors of a whole vehicle body structure, are analyzed as in Fig. 9 and Fig. 10, respectively. The boundary condition is assumed as the free condition. The natural frequencies of each vehicle model are listed in Table 9. The rigid model has about 22% errors, while the CJM model has the negligible errors within 4% in both the bending and the

Table 8 The number of DOFs for the joint area of vehicle body structure

	Shell model	Rigid model	CJM model
Total number of DOFs	2803	2103	1947

Table 9 Natural frequency (Hz) of vehicle body structure

	Shell model	Rigid model	CJM model
Bending mode	40.70	49.80 (22.36%)	39.13 (−3.86%)
Twisting mode	41.61	50.84 (22.18%)	39.88 (−4.16%)
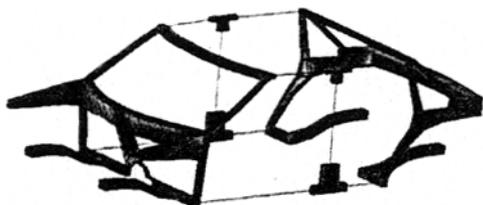
Fig. 8 A detailed vehicle body structure with the shell elements
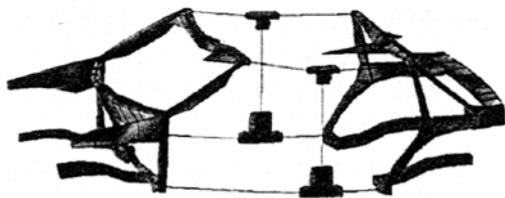
Fig. 9 Overall bending mode shape of vehicle body structure

Fig. 10 Overall twisting mode shape of vehicle body structure

twisting mode.

As expected, the rigid model has much larger dynamic stiffness than shell model. It is confirmed that the CJM model provides strong correlation with shell model in natural frequencies and mode shapes.

8. Conclusion

In this study, a practical method for identifying and expressing the joint characteristics in complete matrix form is presented. The calculations of displacements corresponding to pre-assigned loads are not necessary in this method.

Whatever complex cross sections and curvature may be, the joint characteristics of the vehicle body structure can be very easily expressed in the condensed matrix form. A joint stiffness matrix was derived. It seems that this method would be considerably useful and practical, when not only the static analyses of a vehicle body structure, but also the dynamic analyses are involved. The usefulness of this approach is confirmed by the various example problems including the body structure of the passenger vehicle.

References

Chang, D. C., (1974), "Effect of Flexible Connections on Body Structural Response," SAE Transactions, Vol. 83, pp. 233~244.

Guyan., R. J., 1965, "Reduction of Stiffness and Mass Matrices," *AIAA Journal* Vol. 3, No. 2.

Katakami Tetsufumi, Sugamori Isao, Takahashi Kunihiro, Shimomaki Kazunori, Komatsu Keiji, Tachikawa Katsujiro, Ninomiya Osamu, Maeno Yoshinori, Egashira Yuji and Ono Hyroyuki, 1990, "Joint Stiffness of Body Structures - Part 2 Joint stiffness of L-, T-, Y-type Joints -," *JSAE*, No. 43, pp. 143~147.

Kim Yoon Young, Yim Hong Jae, Kang Jeong Hoon and Kim Jin Hong 1995, "Reconsideration of the Joint Modeling Technique: In a Box-Beam T-Joint," SAE Paper No. 951108, pp. 275~279.

Maurice Petyt, 1980, "Introduction to Finite Element Vibration Analysis," Cambridge pp. 364 ~369.

Moon, Y. M., Jee, T. H. and Park, Y. P., 1995, "Joint Stiffness of Automotive Structural Model,"

the '95 KSME Spring Conference, Vol. 1 pp. 701 ~706.

Shimomaki Kazunori, Sugamori Isao, Takahashi Kunihiro, Komatsu Keiji, Tachikawa Katsujiro, Ninomiya Osamu, Katakami Tetsufumi, Maeno Yoshinori, Egashira Yuji and Ono Hiroyuki, 1990, "Joint stiffness of Body Structures - Part I Its Evaluation Method -," *JSAE*, No. 43, pp. 138~142.

Wright, G. C. and Miles, G. A., 1971, "An Economical Method for Determining the Smallest Eigenvalues of Large Linear Systems" *Int. J. Num. Meth. Eng. 3*, pp. 25~34.